Journal of Environmental Radioactivity 223–224 (2020) 106400

Contents lists available at ScienceDirect

Journal of Environmental Radioactivity

journal homepage: http://www.elsevier.com/locate/jenvrad

Near real-time soil erosion mapping through mobile gamma-ray spectroscopy

Adam Varley *, Andrew Tyler, Clare Wilson

Department of Biological and Environmental Sciences, University of Stirling, Stirling, FK9 4LA, United Kingdom

ARTICLE INFO

Keywords:
Soil erosion
Tillage
Mobile gamma-ray spectrometry
Caesium-137

ABSTRACT

Soil erosion has been associated with various negative environmental impacts foremost of which is the potential pressure it could impose on global food security. The poor conditions of our agricultural soil can be attributed to years of unsustainable farming practices occurring throughout history that has placed significant pressure on the environment. Moreover, climate change scenarios indicate further intensification which is likely making prediction and assessment of erosion processes critical for long term agricultural sustainability. This study demonstrates the potential of mobile gamma-ray spectrometry with large volume NaI(Tl) detectors to identify, at high spatial resolution, changes in ^{137}Cs soil concentration within the ploughed layer of soil and enabling the soil erosion processes to be quantified. This technique represents a significant advantage over conventional spatially-isolated point measurements such as soil sampling as it offers real time mapping at the field scale. However, spectral signal derived from measurements in the field are highly dependent on the calibration procedure used and are particularly sensitive to source-detector changes such as the presence of a vehicle, ground curvature and soil moisture content. Conventional calibration procedures tend to not consider these potential sources of uncertainty potentially leaving the system vulnerable to systematic uncertainties, especially when 137Cs concentrations are low. This study used Monte Carlo simulations to investigate such changes utilising additional information including a high-resolution digital terrain model. The method was demonstrated on a ploughed site in Scotland, revealing a mixture of tillage and water erosion patterns supported by soil core data. Findings showed that the sites topography had relatively little effect (<10%) on calculated erosion rates, but moisture content could be the determining factor, albeit very difficult to measure reliably throughout a survey.

1. Introduction

1.1. Issues of soil erosion

Soil erosion is a global issue, known to be associated with significant negative environmental impacts including increased flooding risk and pollutant migration (Guerra et al., 2017). Losses of fertile top soils and reduced agronomic productivity has been recognised as one of the principal threats to global food security as approximately 90% of the world's foods are grown on this fragile natural resource (Amundson et al., 2015; Pimentel, 2006). In the second half of the 20th century soil erosion globally is thought to have intensified by sustained agricultural land expansion and intensification of farming practices, in particular tillage (Montgomery, 2007). Tillage removes surface vegetation cover exposing soil to rainsplash and overland flow, it also physically damages aggregates and reduces soil organic matter making it more susceptible to water and wind erosion (Morvan et al., 2018). Furthermore, tillage on slopes leads to the physical movement of soil downslope with gravity, with characteristic loses on convexities and accumulation in concavities (Van Oost et al., 2006). In regions that are dominated by arable agriculture, tillage-erosion significantly increases soil erosion rates (Boardman, 2006). At the current rate of erosion, conservative estimates predict that within the next 60 years the productivity of top soils around the globe could be significantly impacted, with areas of agricultural activity worst affected (Foucher et al., 2014).

Over the past century, there have been concerted efforts to better understand the processes that underpin soil erosion (Boardman, 2006). Soil scientists have quantified the erodability of different soils under different environmental settings, enhancing our understanding of how topography influences soil movement and have gone some way towards defining the complex interactions of these processes with meterological and climatic conditions and human pressures (Guerra et al., 2017). This

* Corresponding author.
E-mail address: a.l.varley@stir.ac.uk (A. Varley).

https://doi.org/10.1016/j.jenvrad.2020.106400
Received 1 June 2020; Received in revised form 5 August 2020; Accepted 24 August 2020
Available online 13 September 2020

research has underpinned the development of a range of soil erosion models to predict soil erosion rates on a variety of spatial scales. Using a modelling approach, large areas can be characterised relatively inexpensively often using freely available data. In comparison field-based measurements can be small-scale, expensive, time consuming and often spatially unrepresentative (Borrelli et al., 2017). Successful application and validation of water-mediated soil erosion models has been performed on varying spatial scales (Panagos et al., 2014). However, the regional applicability of these models is often limited and data to validate the models is sparse (Avwunudiogba and Hudson, 2019). Tillage-induced erosion is addressed in models such as WATEMSEDEM (Van Oost et al., 2006), TELEM (Vieira and D.S.M., 2009) and TILLEM (Li et al., 2007), but often with limited success. These models rely on land use histories, which may partially be derived using hyperspectral satellite data (Borrelli et al., 2017), although estimates are typically limited by the issues around spatial and temporal resolution. However, plough speed, direction, depth and frequency are rarely recorded, hence ploughing practices are generally assummed to be relatively uniform in these models making it difficult to assess the real impact of soil erosion with tillage practice at the field-scale (Borrelli et al., 2018). Inevitably, further development of technologies such as LIDAR measurements, drone photogrammatry and satellite imagery will play a bigger role in the assessment of future soil erosion. Nevertheless, the analysis and quantification of historic soil erosion still represents a significant challenge.

1.2. Assessing soil erosion through ^{137}Cs

The most prevalent method to estimate how much soil erosion has taken place is through the use of fallout radionuclides (Walling, 1998; Lobb et al., 1999; Porto et al., 2014). Fallout radionuclides can be found in almost any environmental system and are present as a result of atmospheric wet and dry deposition (Alewell et al., 2017). For example, ^{7}Be and ^{210}Pb, both naturally occurring fallout radionuclides, have been used to assess respective short and medium time scale soil movements (L Mabit et al., 2008). To date, the anthropenic radionuclide ^{137}Cs is the most widely researched medium-term soil tracer and it has been applied across landscapes at varying spatial scales (Evans et al., 2017; Gaspar et al., 2013; Golosov et al., 2018; Owens et al., 1997; Tyler and Heal, 2000).

Over 90% of the global inventory of ^{137}Cs originated from atmospheric nuclear weapons testing carried out during the late 1950's into the early 1960's before the Partial Nuclear Test Ban Treaty was signed in 1963 (Ritchie and McHenry, 1990). It is thought that the vast majority of the ^{137}Cs released into the environment during atmospheric weapons testing was forced high into the atmosphere, where it was well mixed. Subsequently, a relatively uniform deposition of ^{137}Cs occurred on a regional scale compared to more heterogeneous deposition events such as Chernobyl and Fukishima Dia-chi driven by local metereological conditions (Mabit and Dercon, 2014; Varley et al., 2017). Evidence has been put forward by a selection of studies most notably Parsons and Foster (2011) questioning the viability of this assumption. However, others have disagreed with this assessment and have argued if the necessary precautions are taken when selecting a suitable close-by reference site effects from features such as local microclimates should be avoided (Mabit et al., 2008, 2013; Walling and Quine, 1993).

Caesium is a highly reactive alkali earth metal, therefore shortly after deposition, ^{137}Cs is believed to become strongly adsorbed to soil cation exchange sites such as illite and montmorillonite within the timeframe of minutes to hours (Rigol et al., 2002). It is also strongly absorbed to soil organic matter (Melin et al., 1994). Throughout the scientific community it has become widely accepted that once caesium has bound to the soil it is essentially non-exchangable (Park et al., 2019; Ritchie and McHenry, 1990). The assumption therefore made by soil science studies, is that any redistribution of ^{137}Cs from its original uniform distribution has been caused by soil erosion/deposition processes post 1963 rather than through processes such as chemical remobilisation (Hancock et al., 2019; IAEA, 1998; Reinhardt and Herrmann, 2018; Van Oost et al., 2007) (Fig. 1).

On an agricultural field erosion processed lead to two observations within the soil column. Firstly, a reduction in the depth that ^{137}Cs is found in the plough layer as the plough layer is thinned and material is moved away through a mixture of gravity and lateral movement by the plough. Secondly, as ^{137}Cs is moved away from the area, further bites of the plough often occur into uncontaminated material or the bedrock below the original plough layer, gradually reducing the concentration of ^{137}Cs (Bq Kg^{-1}) as contaminated material is mixed with non-contaminated soil. This effect is most frequently observed on the brow of the hill (Fig. 1).

Caesium-137 can be measured in a number of ways, for example, soil redistribution has been demonstrated at regional scales using gamma-ray spectrometry data derived from aerial surveys (Rawlins et al., 2011), However, for field scale resolution, laboratory gamma-ray spectrometry; a procedure that is customarily performed on soil samples extracted incrementally down the profile of a soil core that has been extracted from a site, is commonly used (Owens et al., 1997). The total inventory is then calculated for a number of cores, typically placed strategically along the slope sequence, and a soil erosion rate for individual cores is determined with respect to a core taken from a flat stable area, or reference site, close to the study site (He and Walling, 2000). This methodology has become the standard way to measure soil erosion (Gaspar et al., 2013). Nonetheless, assessing ^{137}Cs through this method is a labour-intensive and time-consuming process that involves a large amount of costly laboratory work. Moreover, many have argued that results could be susceptible to bias due to local heterogeneities in ^{137}Cs (Parsons and Foster, 2011; Sutherland, 1991).

1.3. Field gamma-ray spectrometry

Field gamma-ray spectrometry provides a viable solution to address the issue of minor spatial heterogeneities by averaging out small scale differences given that a large cross section of soil is remotely measured, rather than extracting perhaps less representative soil samples (Davidson et al., 1998; He and Walling, 2000; Wilkinson et al., 2006). Nevertheless, this approach has been little explored since these early investigations and there is also insufficient evidence in the literature as to why, but this may be due to the low counting efficiencies associated with the high-purity germanium detectors used in the original surveys. This would have resulted in long count times and overall poor spatial coverage, an outcome that is arguably not a significant improvement on the speed of coring, albeit without the demands and expense of laboratory analyses.

In this study, we propose using much larger inorganic scintillation

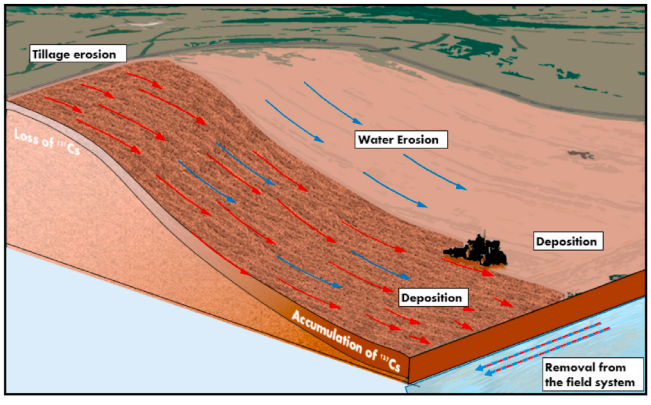

Fig. 1. Process of tillage and water erosion and corresponding erosion and accumulation of ^{137}Cs.

detection crystals made out of sodium iodide (NaI(Tl)) mounted on a vehicle; otherwise known as Mobile Gamma-ray Spectrometry (MGS). Substantially higher counting efficiency can be achieved using this detection setup when compared to the smaller stand-operated HPGe detectors used in previous erosion studies (e.g. Tyler and Heal, 2000). However, this comes at the cost of significantly reduced energy resolution, which often requires sensitive spectral processing routines in order to deconvolute spectral signal components. Similar systems such as the MEDUSA (van der Graaf et al., 2007) and Groundhog systems (Davies et al., 2007) are already well established and employed around the world to measure environmental radioactivity in a number of different scenarios and for a number of different purposes. Such examples include soil texture identification (Heggemann et al., 2017; Priori et al., 2014; Van Der Klooster et al., 2011), search for "hot" particles (Aage and Korsbech, 2003; Dowdall et al., 2012; Long and Martin, 2007; Tyler et al., 2010) and dispersed radiation contaminant mapping (Tanigaki, 2014). At the present time, no ground-based mobile system exists that has been tailored for the assessment of soil erosion using ^{137}Cs spatial distribution.

Previous ground-based attempts might have been prevented early in the development stage due to the difficult nature of the measurement. Principally, as a consequence of the low spectral resolution of NaI(Tl), background contributions from ^{40}K and the ^{238}U and ^{232}Th series occurring across the environmental spectral range (0–2614kev), must first be quantified and then "stripped" out to leave only ^{137}Cs contributions in the 662 keV region (Tyler, 2008). Across much of the environment, atomic weapons testing ^{137}Cs concentrations tend to be low and regularly presents a relatively small signal in comparison to background contributions. The uncertainty introduced by the stripping procedure from both random and systemic components result in a high noise to signal ratio (Allyson and Sanderson, 2001). Some of the random counting uncertainty, introduced by the short acquisition times in modern surveying techniques, can be suppressed using post-processing statistical techniques such as Noise Adjusted Singular Value Decomposition (NASVD) or Maximum Noise Fraction (MNF) (Dickson, 2004).

NASVD has been found to suppress noise within MGS surveys and is utilised within this study (Hovgaard and Grasty, 1997). Highly correlated behaviour between energy bins, occurring across a spectral data set, can be estimated using orthogonal transformations to maximise covariance. Importantly, data must first be scaled to account for the noise structure brought about by count data (Hovgaard, 1997). The resulting rescaled uncorrelated principal components are produced with lower order components accounting for more variation than higher ones. It is assumed most of the real signal is contained within the first 6–10 components for a typical survey, enabling the surveyor to use only these lower order components to reconstruct a cleaner data set and calculate windows (Mauring and Smethurst, 2005).

Another significant challenge faced when attempting to infer any soil radionuclide concentrations using MGS are spectral changes brought about by the presence of the vehicle, ground curvature and changes in soil moisture content (Reinhardt and Herrmann, 2018). Such changes are difficult to account for in standard stripping matrices and relatively little effort has been put forward to try and investigate this occurrence for MGS (Boson et al., 2008; de Groot et al., 2009). In the majority of studies, researchers tend to utilise a set of stripping coefficients derived using concrete calibration pads (Allyson and Sanderson, 2001) or in a few cases using in field calibration techniques (Caciolli et al., 2012). These methods do not always include the vehicle that the detectors are mounted on which could shield photons originating from the ground (Tanigaki, 2014). Furthermore, calibration pads or selected calibration sites are intended to be flat, a scenario that is rarely encountered in a large proportion of agricultural fields, particularly those that are steep and potentially the most sensitive to erosion. In this scenario, significant changes to spectral shape could render stripping ratios invalid leading to under or overestimations of radionuclide. Curvature of the ground can also potentially lead to a change in field of view of the detector, leading to an increased total signal in concavities and introducing an element of shielding in convexities. Therefore, it seems necessary to investigate this behaviour for a detection system and see whether it is possible to account for this effect using dynamic stripping ratios that are reactive to the underlying mapping information provided by high resolution Digital Terrain Models (DTMs). Monte Carlo simulations offer the only practical means of assessing geometric uncertainties such as the presence of a vehicle (Malins et al., 2015), curvature of the ground and moisture content. This type of uncertainty analysis is not typically performed, which is crucial to assess the uncertainty of MGS estimates of ground activity concentration (Persson et al., 2018; Sowa et al., 1989).

This study aims to design and assess the performance of a car-borne gamma-ray system for application of measuring the redistribution of low concentrations of ^{137}Cs across field systems to infer soil redistribution through tillage and erosion. Changes in spectral shape and magnitude brought about by vehicle, ground curvature and moisture content will also be investigated and applied to an agricultural field in Scotland.

2. Methodology

2.1. Case study site and fieldwork

The MGS data was taken in April 2016, with permission of the landowner, from an agricultural field located in the central belt of Scotland (55° 0′ 23.1063″ N, 2° 44′ 37.3379″ W) (Fig. 2). This area of Scotland was known to have little influence of Chernobyl fallout (Tyler and Copplestone, 2007) yet still have enough ^{137}Cs (~3 kBq m^{-2}) from atomic weapons testing mostly from the early 1960's to still be measurable (Fig. S5) (Wright, 2016). The field site is located next to a protected archaeological site and although nothing of archaeological significance had ever been found in the field of study, for caution the farmer had maintained a plough depth of approximately 20 cm for the past 30 years to minimise the influence on deeper features that could potentially be below the surface. At the time of measurement, the field was in pasture but had been regularly ploughed on a 5-year rotation, one year in crop and four years in pasture, for more than 30 years. Five cores were taken along a section of the site enabling ^{137}Cs inventories to be derived from soil concentrations through laboratory gamma-ray spectrometry (Fig. 2). This field study site will be refered to as Roughcastle for the rest of the manuscript.

2.2. Hardware and software

The mobile gamma-ray spectometry system comprised of two 4 L (10.16 × 10.16 × 50.8 cm) NaI(Tl) detectors (Model 2 × 4H16/3.5, Saint Gobain, Nemours, France), attached to Hamamatsu photomultiplier tubes and powered and controlled by a Digibase multichannel analyser made by Ortec. Each detector was housed in durable plastic Pelicases and contolled via a USB port with Ortec's Maestro software. Spectral data containing 1024 channels between 0 and 3000 keV with acquisition times of 1 s. Ortec's gain stabilisation was centred on the 1460 keV ^{40}K peak during survey to reduce the effect of spectral drift. Concurrently, GPS data was collected using an SXblue II device and combined each second with time stamped spectral data. All data was combined using an in-house JAVA program named Mobile Gamma Spectrometry System (MoGSS) developed by the University of Stirling with funding from the Scottish Environment Protection Agency.

Detectors were attached to a bike rack mounted on the towbar of 4 × 4 pickup truck (Fig. 3). The detectors were kept at a constant height of 0.5 m from the ground and a driving speed of 2 m s^{-1} was maintained throughout the survey. Detectors were mounted off the back of the truck rather than a conventional roof-rack mounting for two reasons. Firstly, to ensure there was minimum shielding from the vehicle. Secondly, to reduce the field of view (FOV) of the detector to maintain enough spatial sensitivity to potentially resolve small scale variations.

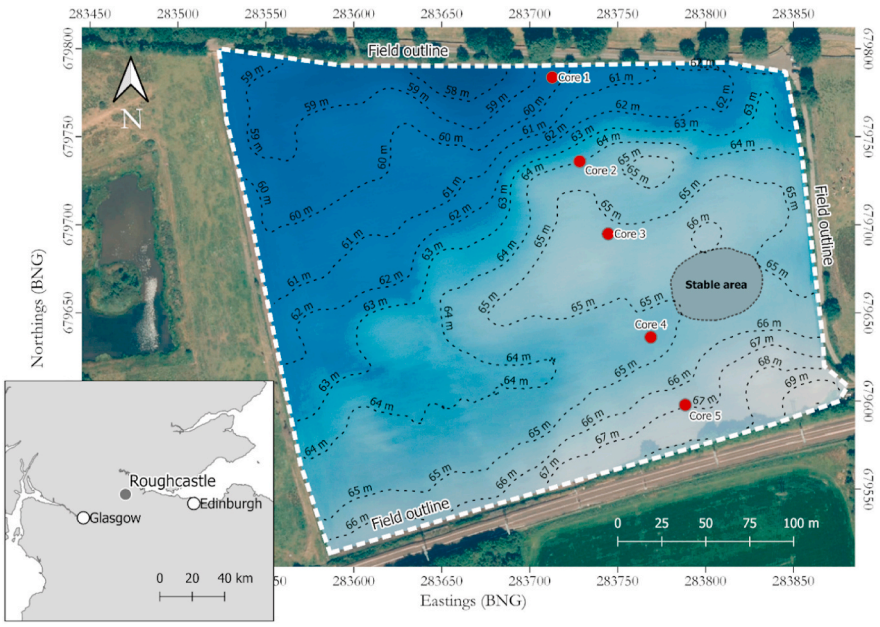

Fig. 2. Overview of Roughcastle site including stable area, core locations (red circles) and topography. (For interpretation of the references to colour in this figure legend, the reader is referred to the Web version of this article.)

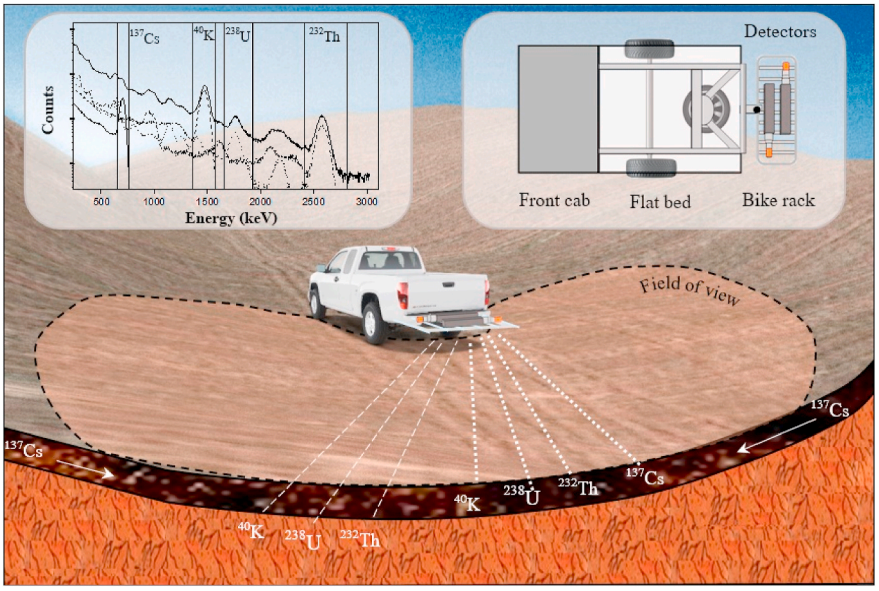

Fig. 3. Schematic diagram of the mobile gamma-ray spectrometry system used to measure ^{137}Cs concentration. Individual spectral responses to ^{137}Cs, ^{40}K, ^{238}U and ^{232}Th (top left) and birds-eye view of the geometry modelled in Monte Carlo simulations to derive spectral responses (top right).

2.3. Processing of field data

NASVD was performed on raw spectra prior to windows counts being derived in an attempt to suppress some of the counting noise present within individual windows (Hovgaard, 1997). The procedure outlined by Mauring and Smethurst (2005) was followed to transform and reconstruct the spectral dataset. Signal was assumed to be in the top 10 spectral components, therefore lower order components were not used to reconstruct spectra as they were assumed to contain predominantly noise. Counts were then extracted from the transformed dataset using windows between the energies for 2405–2800 keV for thorium (W_T), 1660–1927 keV for uranium (W_U), 1366–1578 keV for potassium (W_K) and 657–762 keV for caesium (W_{Cs}) (Fig. 4). The final count rate matrix was then ready for spectral stripping using the appropriate stripping matrix.

2.4. Stripping coefficients

Stripping coefficients derived from Monte Carlo Simulations (MCS) were used to separate individual contributions from ^{40}K and the ^{238}U and ^{232}Th series allowing for ^{137}Cs signal to be isolated (Eqs. (1)–(4)). Stripping coefficients α, β, γ, a, b and c were calculating by taking the ratio between windows (W_T, W_U, W_K and W_{Cs}) taken from calibration spectral datasets both for MCS and concrete calibration pad data. The procedure and nomenclature outlined in IAEA (1991) was followed. Where N' is raw window counts and N is stripped window counts for a given window from the MCS.

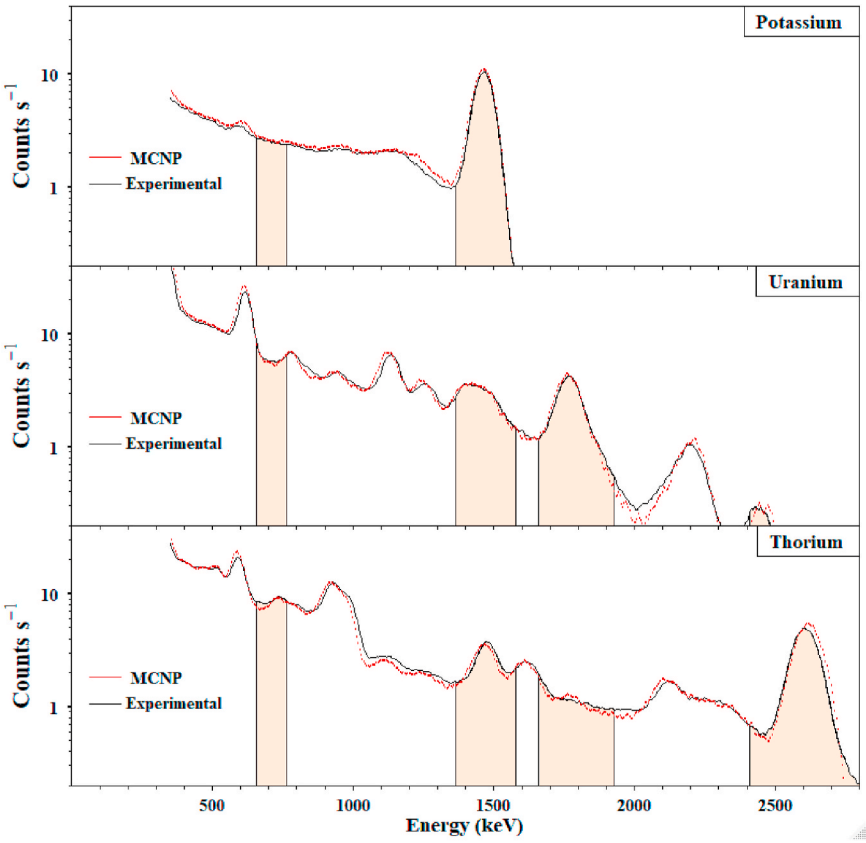

Fig. 4. Benchmark experiments: spectra obtained on ^{40}K, ^{238}U and ^{232}Th on 1 × 1 × 0.3 m concrete calibration pads (black lines) compared to MCNP spectra (red lines) in a simulated geometry. Windows are also plotted for visual reference. (For interpretation of the references to colour in this figure legend, the reader is referred to the Web version of this article.)

$$N_{Th} = N'_{Th} \quad (1)$$

$$N_U = N'_U - \alpha N'_{Th} \quad (2)$$

$$N_K = N'_K - \beta N'_U - \gamma N'_{Th} \quad (3)$$

$$N_{Cs} = N'_{Cs} - a N' - b N'_U - c N'_{Th} \quad (4)$$

Stripped window counts for ^{137}Cs (N_{Cs}) could then be converted into ground activity estimates by dividing by the activity normalised count rate in the W_{Cs} taken from the ^{137}Cs calibration spectrum.

2.5. Converting ^{137}Cs soil concentration to soil erosion rate

Ground activity point estimates for ^{137}Cs were then spatially smoothed using ordinary kriging to produce a uniform raster at 1 m^{-2} (Ciotoli et al., 2017). The R software package 'automap' was used to perform kriging, the software also automatically chose a spherical model fit for the semivariogram (Hiemstra et al., 2008). A flat area towards the south east of the site (Fig. 2) was utilised as a stable area and the average concentration of ^{137}Cs within this area was then used to determine the erosion rate (E), in mm yr^{-1}, for all of the other pixels (Eq. (5)). Where M was the estimated plough layer depth (in mm) derived from soil cores, C_i the concentration of ^{137}Cs at point I in Bq m^{-2}, C_r the concentration of ^{137}Cs within the stable site in Bq m^{-2} and n the number of years since deposition (1963 was adopted as it was the maximum year of input from weapons testing). The observable plough layer depth is different to the plough depth reached by the ploughing instrument as accumulation or erosion events over many years can vary the thickness of this layer. The exact plough layer depth at any one point is difficult to determine and can only be determined through soil coring or soil pits which are labour intensive and arguably not representative of the entire field, therefore a standard value of 250 mm for M was adopted across the study site.

$$E = M\left(\frac{C_i - C_r}{C_r}\right)\cdot\frac{1}{n} \quad (5)$$

2.6. Monte Carlo modelling of the mobile gamma-ray spectrometry system

The software package Monte Carlo N-Particle (MCNP) was used to model detector response to changes in environmental conditions (Briesmeister, 1993). A detailed description of the Monte Carlo method is provided in section 1 of the supplementary materials alongside detailed diagrams of the dimensions used to create the truck geometry and detector setup (Fig. S1). The truck's geometry was simplified, but the main components including the chassis, back wheels, flatbed, supporting struts and front cab were all measured by hand and kept to scale. The bike rack and towbar were also modelled, but the plastic Pelicases around the detectors were not as they were thought to contribute negligible shielding material. The method for modelling curvature of the land in MCNP5 is described in detail in section 2 of the supplementary materials.

2.7. Benchmark experiments

Benchmark experiments are critical in the validation of detector codes as extrapolation using an incorrect detector design are likely to introduce erroneous results. Flat concrete calibration pads doped with known amounts of ^{40}K, ^{238}U and ^{232}Th, located at the British Geological Society, were used as the benchmark geometry. Gamma emissions from these radionuclides span the entire energy range (0–2461 keV) that is relevant to environmental gamma-ray spectrometry, negating the need

for a pad doped with ^{137}Cs.

2.8. Deriving curvature from the digital elevation model (DEM)

A high-resolution Digital Elavation Model (DEM) was derived using LIDAR taken by a fixed-wing plane flying at approximately 30 m. The data was captured in 2013 and was supplied by Historic Environment Scotland as part of the survey of the Antonine Wall. Each pixel was approximately 50 mm in size with an estimated height uncertainty of less than 10 mm. There are several off-the-shelf curvature algorithms based off the second derivative of the DEM available in various GIS applications some of which are open source, such as SAGA and GRASS accessible through QGIS. However, their application for this application is limited due to their inability to increase the size of the kernel window to fit the FOV of the detector and at the same time weight the curvature fit the FOV. This is particularly important as most of the counts received by the detectors will be derived from closer to the detector. Subsequently, the spatial kernel should have a stronger influence from areas closer to the detector falling away in an exponential fashion with increasing distance.

For this application a tailored spatial algorithm was written in R (R Core Development Team, 2016). The algorithm was based upon fitting the reciprocal, used to form curvature models in MCNP (section 2 of supplementary material), to the surrounding elevations on the DEM within a 15 m window of a measurement. Importantly, the function was designed to account for the fact that areas of localised curvature would have more influence on the spectrum as more counts would be received from these areas. Fitting of the reciprocal function was therefore weighted according to the drop off in total count rate as a function of distance from the detector.

2.9. Moisture content

To investigate the influence of moisture content on spectral shape and magnitude the procedure outlined by de Groot et al. (2009) was followed. Assessment of moisture was only considered for a flat geometry and the model was again extended to 15 m in the lateral direction. Interestingly, changes in soil moisture content not only change the density of the soil column as air is displaced out of pore spaces, but also the addition of water effectively generates small changes in elemental composition. These two factors are important when defining nuclear cross-sections in MCNP5 for further details refer to section 3 of the supplementary materials.

3. Results and discussion

3.1. Benchmark experiments

Results from benchmark experiments using a controlled 1 × 1 × 0.3 m flat concrete calibration pad demonstrates the reproducibility of the detector geometries coded into MCNP5 (Fig. 4). Observe that the general shape and magnitude of spectra obtained from individual ^{40}K, ^{238}U and ^{232}Th containing concrete calibration data was closely matched by simulated MCNP5 spectra. This provides firm evidence that the MCNP simulations are valid and can be confidently used in further simulations with variations of environmental variables such as changes in surface geometry or soil density.

For the purposes of reproducibility, the raw pad data have not been stripped using the background pad as overstripping was observed. Instead the known quantities of potassium, uranium and thorium in each pad was used in simulation to give only positive spectral results. Enhanced values of uranium series for example at the 609 keV peak were found perhaps owed to radon disequilibrium at the site; a scenario that is difficult to avoid. Critically, conventional concrete calibration pad protocols rely on the background being as stable as possible to derive the correct stripping coefficients. Such a result could lead to overstripping of Wcs, producing unreliable final activity estimates.

3.2. Influence of vehicle on spectral response

A much larger area of soil, spreading out to 15 m in the lateral direction, was used in the remaining simulations. The first investigation was to assess whether the presence of the vehicle brought about any significant spectral changes. To address this the model being run twice, one simulation with the vehicle and one without. Spectral shape analysis was determined by observing the change in stripping ratios between the two measurements (Table 1). To make for a good comparison the percentage change between measurements is used. In general, small differences (typically within ±3%) were encountered. Positive results indicate larger amounts of lower energy scatter. A typical example of this can be seen when comparing the W_{CS} results to the other windows as relatively more scatter off the truck occurs, effectively transferring higher energy photons into this region. Notice that a 12% increase in the W_{CS} is observed for the uranium series, which is unexpected considering the placement of W_{CS} is in a relatively flat region of spectrum with no major interfering peaks from the natural radionuclides (Fig. 4). One explanation for this is that there is more Compton scatter generated by the mid-energy peaks in the uranium series (1400–2000 keV) in turn producing relatively more counts in the W_{CS}, Further investigations into the exact casues of this observation are needed but are out of the scope of this study.

In the case of $W_{K,}$ on the other hand, slightly less counts are observed when the vehicle is in place (Table 1). W_K contains more peaks derived from radioactive daughters of the uranium and thorium series (notably ^{214}Bi and ^{214}Pb). Therefore, in the case of W_K, attenuation of these peaks must have more influence than the presents of scattering contributions from higher energy. Resultantly, a small reduction in W_K is incurred.

In terms of spectral magnitude there is more of a significant reduction in count rate of 7–9%, which can be seen in the change in window and total spectral counts. In summary, these demonstrate the need to conduct comprehensive modelling exercises to account for external features of a detection system particularly the platform it is attached to.

3.3. Influence of curvature on spectral characteristics

The curvature model shows that there is a relatively small, but statistically significant influence on stripping coefficients as a function of curvature. In the case of the W_{CS}, it can be seen that for ground that is quite convex (−2 to −10% curvature), such as the brow of a hill, there is typically an increase of 4% with respect to a flat surface (Fig. S3). For surfaces that are relatively flat (between 0 and -2% curvature), the influence on the counts in the W_{CS} is less (0–2%). Overall, this observation is relatively easy to explain as more of the source is being shielded as the ground curves in a negative direction, resulting in an increase in the amount photons scattered resulting in more photons detected in W_{CS}.

Conversely, in areas that are concave, for example in a hollow, the relationship is more complex. For small values of concavity (0–5%

Table 1
Change in count rate brought about by the presence of the vehicle expressed as a percentage of the clean pad. Top results are difference in normalised stripping ratios, followed by difference in magnitude of the window counts and the total change across the spectrum (total spectral counts).

Parent radionuclide	Diference in window count rate (%)			
	W_T	W_U	W_K	W_{CS}
Thorium	0	1.57 (α)	−2.32 (β)	1.50 (a)
Uranium	–	0	−0.22 (γ)	11.86 (b)
Potassium	–	–	0	3.29 (c)
Caesium	–	–	–	0
Change in window counts	−7.78	−7.88	−8.88	−7.54
Change in total spectral counts	−8.33	−8.51	−8.17	−8.80

curvature), there is a very small decrease in counts in W_{CS} (<1%) that can be explained by generally less shielding as the ground curves upwards. However, when positive curvature becomes more pronounced (5–10% curvature) more scattering is observed. This outcome is possibly as a result of an increase in shielding provided by the vehicle and photomultipliers at the end of the crystals, as much of the source is curved effectively raising the detectors FOV.

The major influence of ground curvature to this type of measurement is due to spectral magnitude rather than spectral shape (Fig. 5). Notice that areas of convexity contribute approximately 10% more counts into W_{CS} up to −5% curvature. Interestingly, this effect will be partially suppressed by an increase scattering into W_{CS} (Fig. S3). In areas of concavity this relationship is more important and is also not significantly counteracted by scattering from higher energy. For instance, at 10% concavity the detector is likely to receive approximately 40% more counts than on a surface that is flat. Results demonstrate that conventional calibration performed on a flat pad might not be suitable when applied to fields with significant curvature. Little difference between the radionuclides was observed as can be seen for ^{232}Th derived from counts in W_T (Fig. 5).

3.4. Influence of moisture content

Analysis of moisture from similar cores taken from agricultural sites across Scotland over the past 30 years illustrate just how variable moisture content can be ranging between 12 and 46% (Fig. 6). Combining this data with results from the simulated moisture content model derived from Monte Carlo simulations, the overall influence on W_{CS} can be observed. From extreme values, over 40% difference in W_{CS} could potentially be observed within the field. Notably, negligible change in spectral shape was encountered in agreement with the study by de Groot et al. (2009) so there is very little influence on stripping ratios and similar percentage fluence reduction was found for the natural radioelements (W_K, W_U and W_T).

3.5. Core results

Cores extracted from the field down the main slope sequence suggest that tillage and water erosion have taken place (Fig. 2). For example, cores 5 and 3 taken at the top of the field and on the brow of the hill, respectively, had lower ^{137}Cs total inventories (2379 and 1990 Bq m^{-2}, respectively) and a slight thinning of the plough layer (Fig. 7). Core 4 clearly demonstrated a thicker plough layer as accumulation was occurring within this region, but with generally lower ^{137}Cs concentration only had the second highest total inventory (2569 Bq m^{-2}). The highest inventory was found in the middle of the slope section (2834 Bq m^{-2}).

Interestingly, a reduction in ^{137}Cs (1553 Bq m^{-2}) was found at the bottom edge of the site; breaking convention for typical tillage erosion patterns with soil normally gathering in these areas. However, the area where the core was taken drained directly into a culvert and was potentially influenced significantly by water erosion, hence the thinning of the plough layer. Core results demonstrated a clear and explainable erosion pattern, yet is was conceded that there was very few data points to make wider conclusions about the site.

3.6. Application of models to roughcastle

The developed curvature model was applied to the DEM and used to correct counts in W_{CS} to derive final activity and in turn erosion estimates for the Roughcastle survey (Fig. 8). The difference is relatively small, but does change the outcome on erosion calculations in certain areas, noticeably skewed towards losses in count rate induced by areas of convexity such as the brow of the hill. Overall there is very little influence of curvature at this site with a maximum range of −10 to 10%, although the Roughcastle site is reasonably flat compared to other sites in this area.

It is clear from these results that moisture content has the greatest potential to influence MGS estimates of ^{137}Cs concentration and can introduce large uncertainty (Fig. 6). Moisture content is challenging to

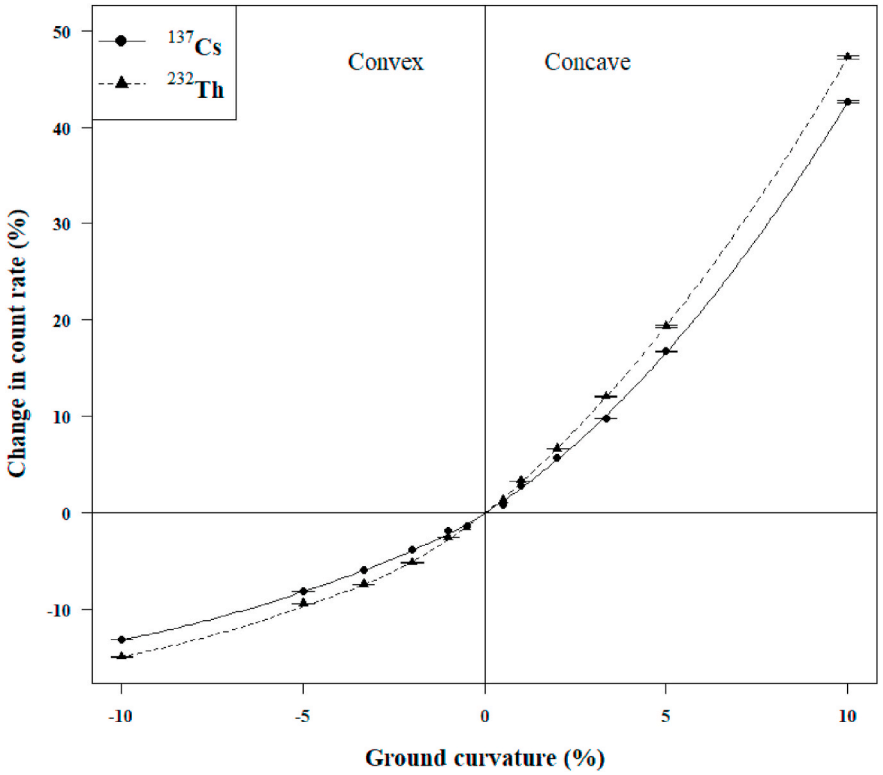

Fig. 5. Percentage change in count rate within thorium (W_T) and caesium (W_{CS}) windows as a function of ground curvature (%).

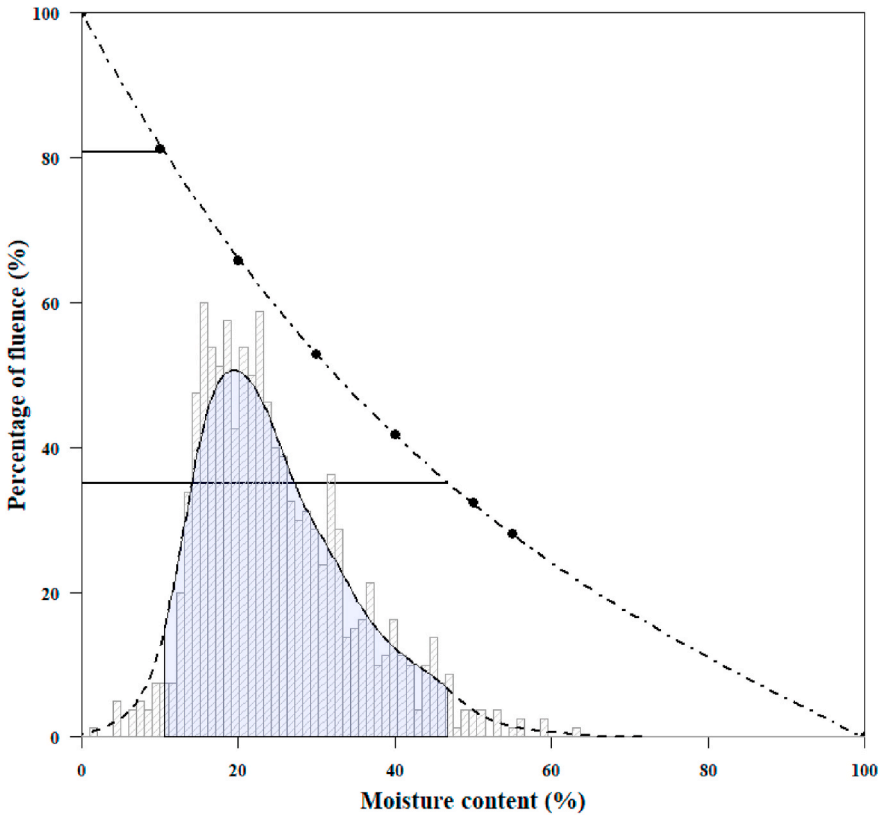

Fig. 6. The percentage influence on fluence in W_{Cs} brought about by changes in soil moisture content. Histogram of approximately 500 moisture content readings within agricultural fields in Scotland. A density function with a 95% of the population is shaded and related to percentage variation in ^{137}Cs signal.

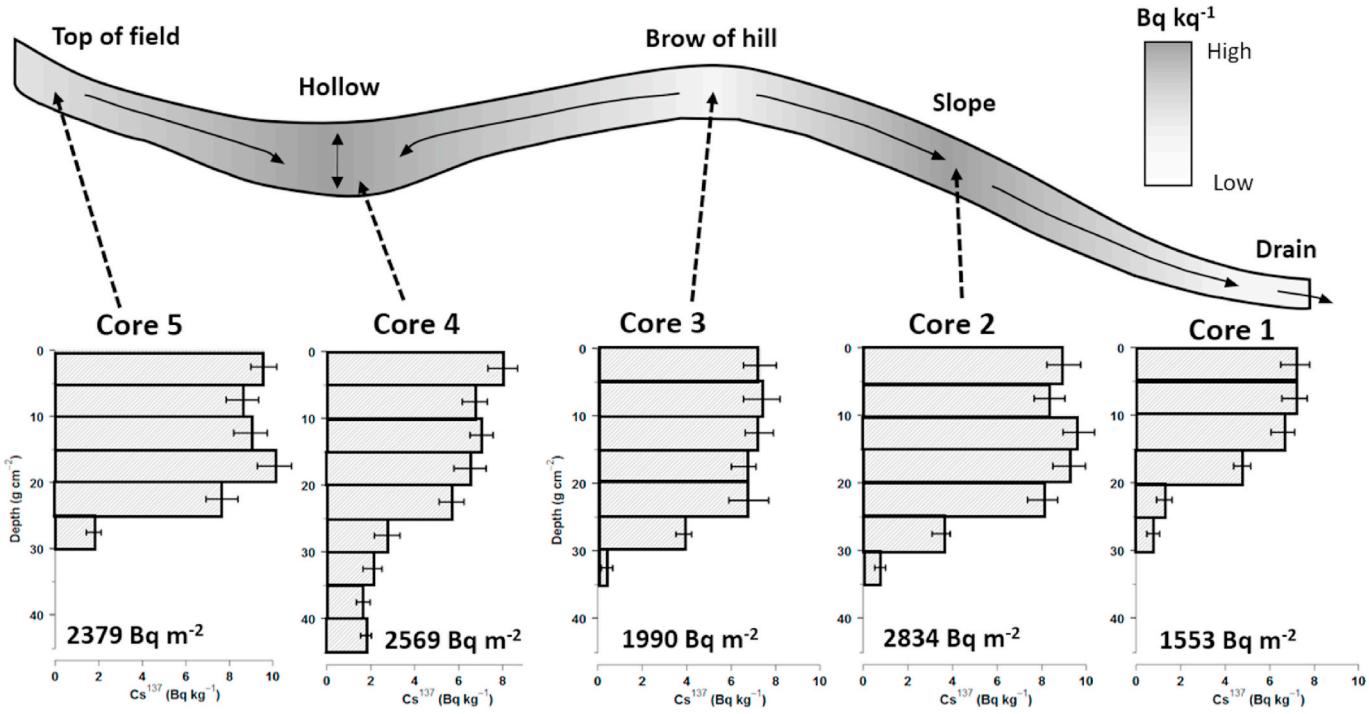

Fig. 7. Caesium-137 core profiles along a section of the Roughcastle site showing redistribution down the slope. Total inventories are noted at the bottom of each profile and error bars indicate counting uncertainty.

reliably measure across a site given that changes can occur over varying temporal and spatial scales. Therefore for countries such as Scotland it is imperitive that surveys are undertaken at specific times of the year when there has been little rainfall over the preceeding few weeks. This was the case during the Roughcastle survey, however a 10% variation was still witnessed across the site using basic soil moisture probe readings and

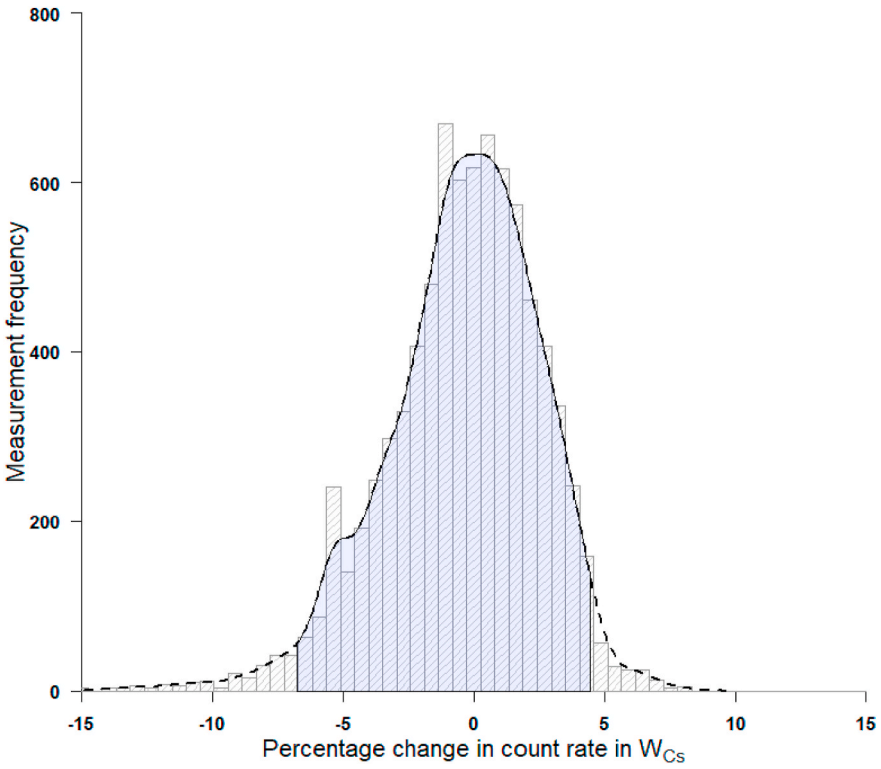

Fig. 8. Influence on count rate in W_{CS} brought about by curvature calculated from the digital elevation model. The shaded area donates 95% of the population.

core data.

3.7. Interpretation of erosion processes occurring at roughcastle

MGS data reveal that higher concentrations of ^{137}Cs had accumulated in the main area of concavity suggesting tillage erosion had taken place at the site (Fig. 9). Conversely, on the brow of the hill and towards the bottom of the site there is significantly less ^{137}Cs in the soil. The observed pattern in ^{137}Cs distribution is more than likely to be a combination of water and tillage erosion that has acted at the site over many years. For comparison, modelled RUSLE and tillage (TillEM) erosion results have been combined, giving a similar erosion pattern across the field providing further support for a mixture of erosion processes. These results do follow the general pattern of the core results, albiet with exeption of the highest core inventory (core 2) observed in the middle of the slope. This could potential be a soil moisture issue in the gamma-ray spectrometery results but is more likely to be a spatial anamoly in the core data comparing to both both modelling and MGS results. This latter point highlights the issue with working with spatially sparse data such as core measurements and supports that application of both methods to try and better determine the erosion history of a site.

The coherence between the mocelling results and MGS techniques, on a raster pixel by pixel basis, is low with a correlation of 0.44 and contribution ratio of 0.19. Yet a general linear trend is observed between the two erosion rates (Fig. S4). Making direct comparisons between the two approaches is difficult as neither is the 'gold standard' for measuring soil erosion and further soil coring was not performed. Clear deviations can be seen at the front of the field where higher areas of accumulation were predicted from the modelling output compared to the MGS results (Fig. 9). It is thought that in this area of soil could have continued moving out of the field beyond the road, which was not accounted for in model perhaps manifesting as an over estimate in the model. An area that the accumulation rate was likely to be underestimated by the MGS was that of the hollow as a significant proportion of contamination was below 20–25 cm (core 4) where the signal at the surface would be challenging to detect, whereas the modelling was likely to better predict this occurrence more accurately (Fig. 9).

3.8. Future prospects

Utilising ^{137}Cs as an environmental tracer has great potential as a tool for retrospective assessment of soil erosion. A tool that could certainly be used in conjunction with emerging technologies such as LIDAR and the latest modelling techniques to develop powerful integrated approaches and to give validation in certain scenarios. However, questions remain over its applicability to the wider environment for the following reasons.

Firstly, within the UK there is significant Chernobyl contributions of ^{137}Cs. Such deposits are known to be highly heterogeneous and many of these regions correspond to regions of high nuclear weapons testing fallout of ^{137}Cs that would otherwise lend themselves well to this type of measurement (Fig. S5) (Wright, 2016). The Roughcastle site was chosen specifically because geographically it is situated in an area that was likely to have enough weapons testing ^{137}Cs inventory (2000–3000 bq m^{-2}) to be detected, but still have relatively low contributions from Chernobyl. A number of other sites in separate regions of Scotland were also measured using this technique, but were demonstrated not to have enough ^{137}Cs to be reliably measured and mapped.

Secondly, the physical half-life of ^{137}Cs is approximately 30 years meaning that only one quarter of the original ^{137}Cs deposited in the 1950's and 1960's remains. Over time this inventory will further decay making it more and more difficult to isolate ^{137}Cs signal from the natural background using *in situ* or MGS. Furthermore, contaminated material below a depth of approximated 20–25 cm is often beyond the limits of detection, thus reducing the sensitivity of the method if contamination is deeply buried particularly in areas of accumation rate. This occurrence was observed in this study in the hollow and led to an underestimation of accumulation rate, although areas of erosion, which could be argued are more important for environmental management, where likely to be predicted with higher certainty.

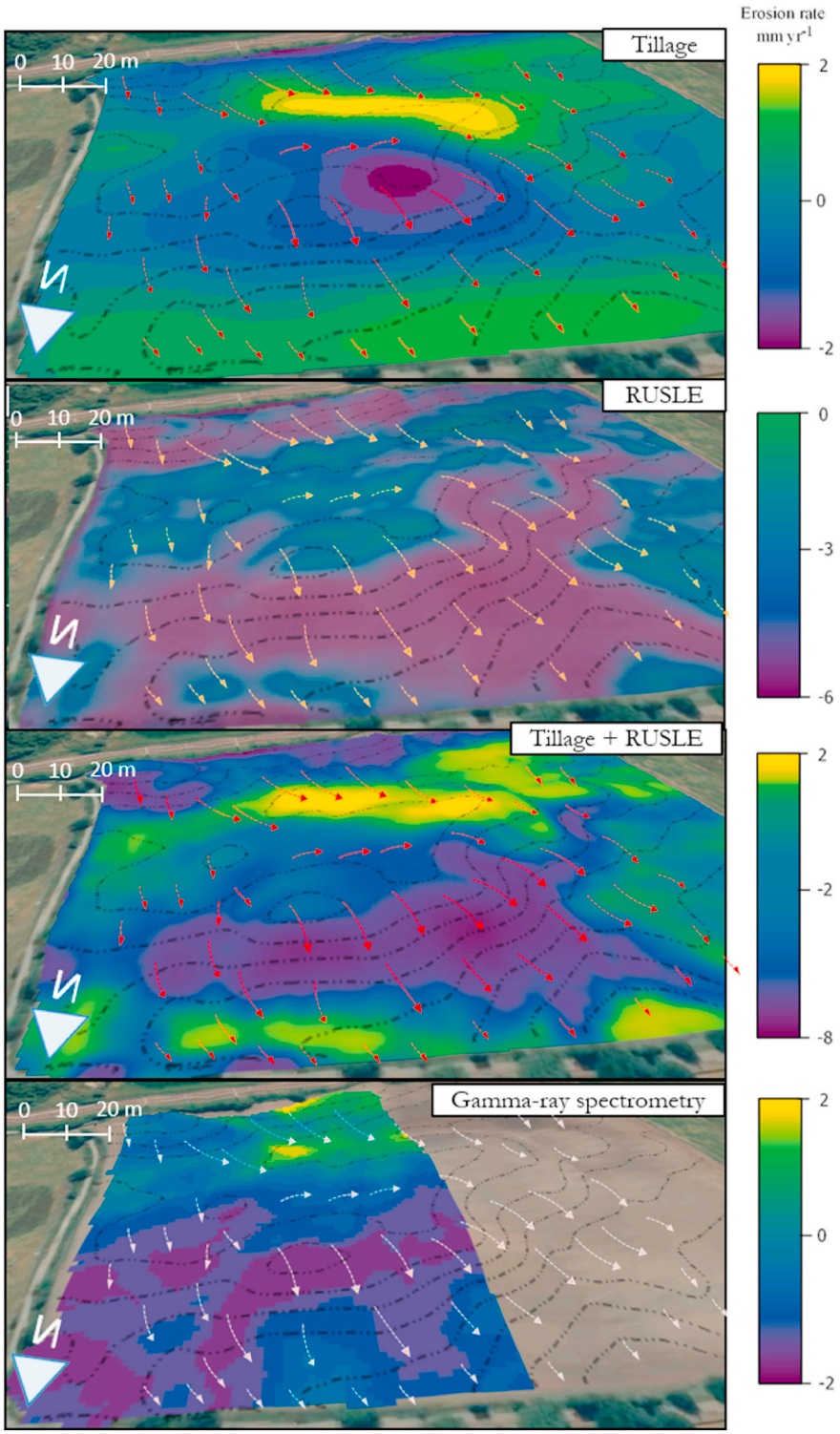

Fig. 9. Erosion rates predicted from a tillage erosion model, RUSLE, combined tillage and RUSLE model and gamma-ray spectrometry. Slope direction arrows have been included.

Finally, remote measurements are not only highly sensitive to changes in soil moisture content, but also any changes in atmospheric radon. During the second half of the Roughcastle survey, a significant proportion of results had to be omitted after a short rain event that led to deposition of the gamma-emitting daughter products of atmospheric radon (notably ^{214}Bi and ^{212}Pb) on the ground surface, which in turn compromised the stripping ratios. These occurrences are very challenging to account for, although some airborne gamma-ray spectrometry surveys have used upward facing detectors to subtract additional contributions (Grasty et al., 1997).

In summary, very specific conditions have to be met in order to be able to get reliable readings in the field. At present large volume sodium iodide detectors offer the best option, but better detection technology will be required with high enough energy efficiency and resolution to be able to confidently separate ^{137}Cs signal from the background.

4. Conclusions

Soil erosion has been identified as a significant threat to global food security and has long been associated with various negative environmental impacts. Clearly, development of tools to measure soil erosion is paramount to identify areas that have been significantly affected, so landowners and regulators can make informed decisions regarding remediation measures. Mobile gamma-ray spectrometry offers the potential to measure soil erosion at high spatial resolution using redistribution of ^{137}Cs, lending itself well to field-scale application. Morevover, it has the potential to reveal erosion processes brought about by individual agricultural practices that are other unobtainable through physical models estimates derived purely from the topography.

It was demonstrated that in some circumstances systematic uncertainties could have a significant effect on results, especially if there are large localised topographic or soil moisture content changes taking place at a site. In some cases, a portion of uncertainty could be moderated using additional information such as moisture content readings and DEMs.

However, there remains considerable obstacles to make the methodology viable for widescale field application. For instance, the method would appear to be very site specific and location would have to be carefully researched prior to application to ensure there was enough atmospheric weapons testing deposition of ^{137}Cs and low Chernobyl deposition. Furthermore, improvement in detector technology are required to confidently resolve signal from ^{137}Cs. Currently no suitable detection material can produce high enough energy efficiency whilst providing high enough energy resolution to resolve spectral issues to be able to rapidly and reliably measure the low density of ^{137}Cs in these types of environments.

Declaration of competing interest

The authors declare that they have no known competing financial interests or personal relationships that could have appeared to influence the work reported in this paper.

Acknowledgements

This work was funded through a AHRC grant (AH/N504452/1) as part of the EU project Cultural Landscape risk Identification, Management and Assessment (CLIMA) project. The authors would like to thank Stuart Bradley for his help in field work and laboratory analysis and Richard Varley for his assistance in reviewing.

Appendix A. Supplementary data

Supplementary data to this article can be found online at https://doi.org/10.1016/j.jenvrad.2020.106400.

References

Aage, H.K., Korsbech, U., 2003. Search for lost or orphan radioactive sources based on NaI gamma spectrometry. Appl. Radiat. Isot. 58, 103–113. https://doi.org/10.1016/S0969-8043(02)00222-1.

Alewell, C., Pitois, A., Meusburger, K., Ketterer, M., Mabit, L., 2017. 239+240Pu from "contaminant" to soil erosion tracer_ where do we stand? Earth Sci. Rev. 172, 107–123. https://doi.org/10.1016/j.earscirev.2017.07.009.

Allyson, J.D., Sanderson, D.C.W., 2001. Spectral deconvolution and operational use of stripping ratios in airborne radiometrics. J. Environ. Radioact. 53, 351–363. https://doi.org/10.1016/S0265-931X(00)00141-7.

Amundson, R., Berhe, A.A., Hopmans, J.W., Olson, C., Sztein, A.E., Sparks, D.L., 2015. Soil and human security in the 21st century. Science 80. https://doi.org/10.1126/science.1261071.

Boardman, J., 2006. Soil erosion science: reflections on the limitations of current approaches. Catena 68, 73–86. https://doi.org/10.1016/j.catena.2006.03.007.

Borrelli, P., Robinson, D.A., Fleischer, L.R., Lugato, E., Ballabio, C., Alewell, C., Meusburger, K., Modugno, S., Schütt, B., Ferro, V., Bagarello, V., Oost, K. Van, Montanarella, L., Panagos, P., 2017. An assessment of the global impact of 21st century land use change on soil erosion. Nat. Commun. 8 https://doi.org/10.1038/s41467-017-02142-7, 2013.

Borrelli, P., Van Oost, K., Meusburger, K., Alewell, C., Lugato, E., Panagos, P., 2018. A step towards a holistic assessment of soil degradation in Europe: coupling on-site erosion with sediment transfer and carbon fluxes. Environ. Res. 161, 291–298. https://doi.org/10.1016/j.envres.2017.11.009.

Boson, J., Nylon, T., Hunell Plamboeck, A., Agren, G., Johansson, L., 2008. Improving Accuracy of in Situ Gamma-Ray Spectroscopy.

Caciolli, A., Baldoncini, M., Bezzon, G.P., Broggini, C., Buso, G.P., Callegari, I., Colonna, T., Fiorentini, G., Guastaldi, E., Mantovani, F., Massa, G., Menegazzo, R., Mou, L., Alvarez, C.R., Shyti, M., Zanon, A., Xhixha, G., 2012. A new FSA approach for in situ ? ray spectroscopy. Sci. Total Environ. 414, 639–645. https://doi.org/10.1016/j.scitotenv.2011.10.071.

Ciotoli, G., Voltaggio, M., Tuccimei, P., Soligo, M., Pasculli, A., Beaubien, S.E., Bigi, S., 2017. Geographically weighted regression and geostatistical techniques to construct the geogenic radon potential map of the Lazio region: a methodological proposal for the European Atlas of Natural Radiation. J. Environ. Radioact. 166, 355–375. https://doi.org/10.1016/j.jenvrad.2016.05.010.

Davidson, D.A., Grieve, I.C., Tyler, A.N., Barclay, G.J., Maxwell, G.S., 1998. Archaeological sites: assessment of erosion risk. J. Archaeol. Sci. 25, 857–860. https://doi.org/10.1006/jasc.1997.0223.

Davies, M., McCulloch, G., Adsley, I., 2007. Experience of monitoring beaches for radioactive particles. J. Radiol. Prot. 27, A51.

de Groot, A.V., van der Graaf, E.R., de Meijer, R.J., Maučec, M., 2009a. Sensitivity of in-situ γ-ray spectra to soil density and water content. Nucl. Instruments Methods Phys. Res. Sect. A Accel. Spectrometers, Detect. Assoc. Equip. 600, 519–523. https://doi.org/10.1016/j.nima.2008.12.003.

De Groot, A.V., Van der Graaf, E.R., De Meijer, R.J., Maucec, M., 2009b. Sensitivity of in-situ gamma-ray spectra to soil density and water content. Nucl. Instruments Methods Phys. Res. Sect. A Accel. Spectrometers, Detect. Assoc. Equip. 600, 519–523.

Dickson, B.L., 2004. Recent advances in aerial gamma-ray surveying. South Pacific Environ. Radioact. Assoc. 2002 Conf. 76, 225–236. https://doi.org/10.1016/j.jenvrad.2004.03.028.

Dowdall, M., Smethurst, M.A., Watson, R., Mauring, A., Aage, H.K., Andersson, K.G., Pálsson, S.E., Polsson, S.E., 2012. Car-borne gamma spectrometry: a virtual exercise in emergency response. J. Environ. Radioact. 107, 68–77. https://doi.org/10.1016/j.jenvrad.2011.11.014.

Evans, R., Collins, A.L., Zhang, Y., Foster, I.D.L., Boardman, J., Sint, H., Lee, M.R.F., Griffith, B.A., 2017. A Comparison of Conventional and 137 Cs-Based Estimates of Soil Erosion Rates on Arable and Grassland across Lowland England and Wales. https://doi.org/10.1016/j.earscirev.2017.08.005.

Foucher, A., Bastien, S., Blanes, S., Evrard, O., Lle Simonneau, A., Chapron, E., Courp, T., Cerdan, O., Ne Lefè Vre, I., Adriaensen, H., Lecompte, F., Desmet, M., 6293 Géhco, E. A, 2014. Increase in soil erosion after agricultural intensification: evidence from a lowland basin in France. Biochem. Pharmacol. 7, 30–41. https://doi.org/10.1016/j.ancene.2015.02.001.

Gaspar, L., Navas, A., Walling, D., Machín, J., 2013. Using 137 Cs and 210 Pb ex to assess soil redistribution on slopes at different temporal scales. Catena.

Golosov, V.N., Walling, D.E., Konoplev, A.V., Ivanov, M.M., Sharifullin, A.G., 2018. Application of bomb- and Chernobyl-derived radiocaesium for reconstructing changes in erosion rates and sediment fluxes from croplands in areas of European Russia with different levels of Chernobyl fallout. J. Environ. Radioact. 186, 78–89. https://doi.org/10.1016/j.jenvrad.2017.06.022.

Grasty, R.L., St John Smith, B., Minty, B.R.S., 1997. Developments in the standardization and analysis of airborne gamma-ray data. Fourth decenn. Int. Conf. Miner. Explor 725–732.

Guerra, A.J.T., Fullen, M.A., Jorge, M., do, C.O., Bezerra, J.F.R., Shokr, M.S., 2017. Slope processes, mass movement and soil erosion: a review. Pedosphere 27, 27–41. https://doi.org/10.1016/S1002-0160(17)60294-7.

Hancock, G.R., Kunkel, V., Wells, T., Martinez, C., 2019. Soil organic carbon and soil erosion – understanding change at the large catchment scale. Geoderma. https://doi.org/10.1016/j.geoderma.2019.02.012.

He, Q., Walling, D., 2000. Calibration of a field-portable gamma detector to obtain in situ measurements of the 137Cs inventories of cultivated soils and floodplain sediments. Appl. Radiat. Isot. 52, 865–872. https://doi.org/10.1016/S0969-8043(99)00126-8.

Heggemann, T., Welp, G., Amelung, W., Angst, G., Franz, S.O., Koszinski, S., Schmidt, K., Pätzold, S., 2017. Proximal gamma-ray spectrometry for site-independent in situ prediction of soil texture on ten heterogeneous fields in Germany using support vector machines. Soil Tillage Res. 168, 99–109. https://doi.org/10.1016/j.still.2016.10.008.

Hovgaard, J., 1997. Airborne Gamma-Ray Spectroscopy. Airborne Gamma-Ray Spectrom. Technical University of Denmark, Department of Automation.

Hovgaard, J., Grasty, R.L.L., 1997. Reducing statistical noise in airborne gamma-ray data through spectral component analysis. Proceedings of Exploration 753–764.

IAEA, 1998. Use of 137 Cs in the Study of Soil Erosion and Sedimentation. IAEA-TECDOC-1028. https://doi.org/10.1016/j.cbpc.2013.09.002. Vienna.

IAEA - International Atomic Energy Agency, 1991. Technical Reports Series No. 323: Airborne Gamma Ray Spectrometer Surveying. International Atomic Energy Agency.

Li, S., Lobb, D.A., Lindstrom, M.J., Farenhorst, A., 2007. Tillage and water erosion on different landscapes in the northern North American Great Plains evaluated using 137Cs technique and soil erosion models. Catena 70, 493–505. https://doi.org/10.1016/j.catena.2006.12.003.

Lobb, D.A., Gary Kachanoski, R., Miller, M.H., 1999. Tillage translocation and tillage erosion in the complex upland landscapes of southwestern Ontario, Canada. Soil Tillage Res. 51, 189–209. https://doi.org/10.1016/S0167-1987(99)00037-9.

Long, S., Martin, L., 2007. Optimisation of systems to locate discrete gamma-ray sources within a large search area. J. Environ. Radioact. 94, 41–53. https://doi.org/10.1016/j.jenvrad.2006.12.012.
Mabit, L., Benmansour, M., Walling, D., 2008. Comparative advantages and limitations of the fallout radionuclides 137 Cs, 210 Pb ex and 7 Be for assessing soil erosion and sedimentation. J. Environ. Radioact.
Mabit, L., Bernard, C., Makhlouf, M., Laverdière, M.R., 2008. Spatial variability of erosion and soil organic matter content estimated from 137Cs measurements and geostatistics. Geoderma 145, 245–251. https://doi.org/10.1016/j.geoderma.2008.03.013.
Mabit, L., Dercon, G., 2014. Guidelines for Using Fallout Radionuclides to Assess Erosion and Effectiveness of Soil Conservation Strategies. International Atomic Energy Agency.
Mabit, L., Meusburger, K., Fulajtar, E., Alewell, C., 2013. The usefulness of137Cs as a tracer for soil erosion assessment: a critical reply to Parsons and Foster (2011). Earth Sci. Rev. https://doi.org/10.1016/j.earscirev.2013.05.008.
Malins, A., Okumura, M., Machida, M., Takemiya, H., Saito, K., 2015. Fields of View for Environmental Radioactivity 2–7.
Mauring, E., Smethurst, M.A., 2005. Reducing noise in radiometric multi-channel data using noise-adjusted singular value decomposition (NASVD) and maximum noise fraction (MNF). Geol. Surv. Norway, Rep.
Melin, J., Wallberg, L., Suomela, J., 1994. Distribution and retention of cesium and strontium in Swedish boreal forest ecosystems. Sci. Total Environ. 157, 93–105. https://doi.org/10.1016/0048-9697(94)90568-1.
Montgomery, D.R., 2007. Dirt: the Erosion of Civilization, the Erosion of Civilizations. https://doi.org/10.2135/cropsci2007.10.0001br.
Morvan, X., Verbeke, L., Laratte, S., Schneider, A.R., 2018. Impact of recent conversion to organic farming on physical properties and their consequences on runoff, erosion and crusting in a silty soil. Catena 165, 398–407. https://doi.org/10.1016/j.catena.2018.02.024.
Owens, P.N., Walling, D.E., He, Q., Shanahan, J., Foster, I.D.L., 1997. The use of caesium-137 measurements to establish a sediment budget for the Start catchment, Devon, UK. Hydrol. Sci. Sci. Hydrol. 42.
Panagos, P., Meusburger, K., Ballabio, C., Borrelli, P., Alewell, C., 2014. Soil erodibility in Europe: a high-resolution dataset based on. LUCAS. Sci. Total Environ. 479–480, 189–200. https://doi.org/10.1016/j.scitotenv.2014.02.010.
Park, S.M., Alessi, D.S., Baek, K., 2019. Selective adsorption and irreversible fixation behavior of cesium onto 2:1 layered clay mineral: a mini review. J. Hazard Mater. https://doi.org/10.1016/j.jhazmat.2019.02.061.
Parsons, A.J., Foster, I.D.L., 2011. What can we learn about soil erosion from the use of 137Cs? Earth Sci. Rev. https://doi.org/10.1016/j.earscirev.2011.06.004.
Persson, L., Boson, J., Nylén, T., Ramebäck, H., 2018. Application of a Monte Carlo method to the uncertainty assessment in in situ gamma-ray spectrometry. J. Environ. Radioact. 187, 1–7. https://doi.org/10.1016/j.jenvrad.2018.02.003.
Pimentel, D., 2006. Soil erosion: a food and environmental threat. Environ. Dev. Sustain. https://doi.org/10.1007/s10668-005-1262-8.
Porto, P., Walling, D., Capra, A., 2014. Using 137 Cs and 210 Pb ex measurements and conventional surveys to investigate the relative contributions of interrill/rill and gully erosion to soil loss from a small. Soil Tillage Res.
Priori, S., Bianconi, N., Costantini, E.A.C., 2014. Can γ-radiometrics predict soil textural data and stoniness in different parent materials? A comparison of two machine-learning methods. Geoderma 226– 227, 354–364. https://doi.org/10.1016/j.geoderma.2014.03.012.
R Core Development Team, 2016. R: a language and environment for statistical computing. R A Lang. Environ. Stat. Comput.
Rawlins, B.G., Scheib, C., Beamish, D., Webster, R., Tyler, A.N., Young, M.E., 2011. Landscape-scale controls on the spatial distribution of caesium 137: a study based on an airborne geophysical survey across Northern Ireland. Earth Surf. Process. Landforms 36, 158–169. https://doi.org/10.1002/esp.2026.
Reinhardt, N., Herrmann, L., 2018. Gamma-ray spectrometry as versatile tool in soil science: a critical review. J. Plant Nutr. Soil Sci. 1–19 https://doi.org/10.1002/jpln.201700447.
Rigol, A., Vidal, M., Rauret, G., 2002. An overview of the effect of organic matter on soil–radiocaesium interaction: implications in root uptake. J. Environ. Radioact. 58, 191–216.
Ritchie, J.C., McHenry, J.R., 1990. Application of radioactive fallout cesium-137 for measuring soil erosion and sediment accumulation rates and patterns: a review. J. Environ. Qual. 19, 215–233. https://doi.org/10.2134/jeq1990.00472425001900020006x.
Sowa, W., Martini, E., Gehrcke, K., Marschner, P., Naziry, M.J., 1989. Uncertainties of in situ gamma spectrometry for environmental monitoring. Radiat. Protect. Dosim. 27, 93–101.
Sutherland, R.A., 1991. Examination of caesium-137 areal activities in control (uneroded) locations. Soil Technol. 4, 33–50. https://doi.org/10.1016/0933-3630(91)90038-O.
Tanigaki, M., 2014. Development of a carborne survey system, KURAMA. In: Takahashi, S. (Ed.), Radiation Monitoring and Dose Estimation of the Fukushima Nuclear Accident. Springer Japan, Tokyo, pp. 67–77. https://doi.org/10.1007/978-4-431-54583-5_7.
Tyler, A.N., 2008. In situ and airborne gamma-ray spectrometry. In: Radioactivity in the Environment, Analysis of Environmental Radionuclides. Elsevier, pp. 407–448. https://doi.org/10.1016/S1569-4860(07)11013-5.
Tyler, A.N., Copplestone, D., 2007. Preliminary Results from the First National in Situ Gamma Spectrometry Survey of the United Kingdom. https://doi.org/10.1016/j.jenvrad.2007.01.029.
Tyler, A.N., Heal, K.V., 2000. Predicting areas of 137Cs loss and accumulation in upland catchments. Water. Air. Soil Pollut 121, 271–288. https://doi.org/10.1023/A:1005219009425.
Tyler, A.N., Scott, E.M., Dale, P., Elliott, A.T., Wilkins, B.T., Boddy, K., Toole, J., Cartwright, P., 2010. Reconstructing the abundance of Dounreay hot particles on an adjacent public beach in Northern Scotland. Sci. Total Environ. 408, 4495–4503. https://doi.org/10.1016/j.scitotenv.2010.06.004.
van der Graaf, E.R., Rigollet, C., Maleka, P.P., Jones, D.G., 2007. Testing and assessment of a large BGO detector for beach monitoring of radioactive particles. Nucl. Instruments Methods Phys. Res. Sect. A Accel. Spectrometers, Detect. Assoc. Equip. 575, 507–518. https://doi.org/10.1016/j.nima.2007.02.107.
Van Der Klooster, E., Van Egmond, F.M., Sonneveld, M.P.W., 2011. Mapping soil clay contents in Dutch marine districts using gamma-ray spectrometry. Eur. J. Soil Sci. 62, 743–753. https://doi.org/10.1111/j.1365-2389.2011.01381.x.
Van Oost, K., Govers, G., de Alba, S., Quine, T.A., 2006. Tillage erosion: a review of controlling factors and implications for soil quality. Prog. Phys. Geogr. https://doi.org/10.1191/0309133306pp487ra.
Van Oost, K., Quine, T.A., Govers, G., De Gryze, S., Six, J., Harden, J.W., Ritchie, J.C., McCarty, G.W., Heckrath, G., Kosmas, C., Giraldez, J.V., Marques Da Silva, J.R., Merckx, R., 2007. The impact of agricultural soil erosion on the global carbon cycle. Science 80. https://doi.org/10.1126/science.1145724.
Varley, A., Tyler, A., Dowdall, M., Bondar, Y., Zabrotski, V., 2017. An in situ method for the high resolution mapping of ^{137}Cs and estimation of vertical depth penetration in a highly contaminated environment. Sci. Total Environ. 605–606. https://doi.org/10.1016/j.scitotenv.2017.06.067.
Vieira, D.A.N., Dabney, S.M., 2009. Modeling landscape evolution due to tillage: model development. Trans. ASABE (Am. Soc. Agric. Biol. Eng.) 52, 1505–1521.
Walling, D., 1998. Use of 137Cs and Other Fallout Radionuclides in Soil Erosion Investigations: Progress, Problems and Prospects. Use.
Walling, D.E., Quine, T.A., 1993. Use of caesium-137 as a tracer of erosion and sedimentation: handbook for the application of the caesium-137 technique. In: UK Overseas Development Administration Research Scheme R4579. Energy Technol. Data Exch, vol. 4579.
Wilkinson, K., Tyler, A., Davidson, D., Grieve, I., 2006. Quantifying the threat to archaeological sites from the erosion of cultivated soil. Antiquity.
Wright, S.M., 2016. Predicted Caesium-137 Deposition from Atmospheric Nuclear Weapons Tests. https://doi.org/10.5285/c3e530bf-af20-43fc-8b4b-92682233ff08.